Swansea University
Prifysgol Abertawe

Cronfa
Setting Research Free

Cronfa - Swansea University Open Access Repository

This is an author produced version of a paper published in:
Journal of The Royal Society Interface

Cronfa URL for this paper:
http://cronfa.swan.ac.uk/Record/cronfa48679

Paper:
Li, S., Wang, C. & Nithiarasu, P. (2019). Electromechanical vibration of microtubules and its application in biosensors. *Journal of The Royal Society Interface, 16*(151), 20180826
http://dx.doi.org/10.1098/rsif.2018.0826

This item is brought to you by Swansea University. Any person downloading material is agreeing to abide by the terms of the repository licence. Copies of full text items may be used or reproduced in any format or medium, without prior permission for personal research or study, educational or non-commercial purposes only. The copyright for any work remains with the original author unless otherwise specified. The full-text must not be sold in any format or medium without the formal permission of the copyright holder.

Permission for multiple reproductions should be obtained from the original author.

Authors are personally responsible for adhering to copyright and publisher restrictions when uploading content to the repository.

http://www.swansea.ac.uk/library/researchsupport/ris-support/

Electromechanical vibration of microtubules and its application in biosensors

Si Li, Chengyuan Wang*, Perumal Nithiarasu

Zienkiewicz Centre for Computational Engineering, College of Engineering, Swansea University, Bay Campus, Fabian Way, Swansea, Wales SA1 8EN, UK

Abstract

An electric field (EF) has the potential to excite the vibration of polarized microtubules(MTs) and thus, enable their use as a biosensor for the biophysical properties of MTs or cells. To facilitate the development, this paper aims to capture the EF-induced vibration modes and the associated frequency for MTs. The analyses were carried out based on a molecular structural mechanics (MSM) model accounting for the structural details of MTs. Transverse vibration, radial breathing vibration and axial vibration were achieved for MTs subject to a transverse or an axial EF. The frequency shift and stiffness alteration of MTs were also examined due to the possible changes of the tubulin interactions in physiological or pathological processes. The strong correlation achieved between the tubulin interaction and MT vibration excited by EF provide a new avenue to a non-contacting technique for the structural or property changes in MTs, where frequency shift is used as a biomarker. This technique can be used for individual MTs and is possible for those in cells when the cytosol damping on MT vibrations is largely reduced by the unique features of MT-cytosol interface.

Keywords: Microtubules; electromechanical vibration; elastic moduli, tubulin interaction

---

*Corresponding author. E-mail address: chengyuan.wang@swansea.ac.uk (C. Wang)

1. Introduction

Microtubules (MTs) are fundamental structural elements in the cytoskeleton (CSK) of eukaryotic cells. They provide mechanical support for the shape of cells, form tracks for directed subcellular transport and are part of the spindle apparatus important for cell division [1, 2]. MTs are composed of heterodimer subunits of α and β tubulins which carry unbalanced negative charge [3, 4]. This biophysical property of tubulin endows MTs with the ability to respond to the external electric field (EF) [5, 6].

Vibration of MTs has attracted considerable attention in the last two decades [7-13]. Recently, the electromechanical vibration of MTs was excited by applying an external EF [2], showing the potential of polarized MTs as biosensors in disease diagnosis and health monitoring. It thus becomes essential to gain an in-depth understanding of the electromechanical vibration of MTs subject to an EF [2, 14]. A theoretical study was first conducted to quantitatively described the EF-generated by a vibrating MT [6], which provides a means to detect the vibration of MTs. After that, an optomechanical technique [2] was proposed to probe and more importantly, stimulate the vibration via EF on MTs modelled as one-dimensional structure. However, MTs are actually three-dimensional (3D) discrete structures composed of charged subunits. It is thus of great interest to explore the behaviour of EF-induced vibration of MTs as 3D nanostructures. In existing studies, vibration analyses were carried out for MTs first in the framework of continuum mechanics theory [10, 11]. Subsequently, discrete approaches were developed to account for nanoscale MT structure and its influence on MT vibration [13]. The typical examples are the molecular dynamics (MD) simulations [15-17] and the cost-effective molecular structural mechanics (MSM) model [18].

In this paper, the MSM model [18] is again employed to simulate the vibration of MTs subject to an alternating EF generated by a dipole antenna. The vibration spectra are recorded for MTs for various possible modes. In addition, the correlation between frequency shift and the possible softening/hardening of MTs is quantified demonstrating the potential application of vibrating MTs as biosensors. In addition, a parametric study is also conducted to evaluate the damping effect of surrounding cytosol, which could be greatly reduced by the nanoscale MT-cytosol interface. The paper is organized as follows. The simulation setup, i.e., an MT subject to an alternating EF of dipole antenna is illustrated in Sec.2. The simulation results and corresponding discussions are given in Sec. 3, and the conclusions are drawn in Sec. 4.

2. Model development and vibration excitation

2.1 MSM model for MT structure

In this work, 13-3 MTs are considered as a typical example, which have 13 Proto-filaments (PFs) and helix start S=3 [19] as shown in Fig.1a. The details of the helix nanostructure were characterised by an MSM model [18] in Fig.1b where the blue balls denote α tubulins and the red balls represent β tubulins. In addition, the intra-PF αβ interactions of MTs are modelled as the longitudinal elastic space beams while the inter-PF αα (ββ) interaction are treated as the helical space beams. Following previous studies [16, 18, 20], the small difference in αα and ββ interactions is neglected. Such a frame structure model is developed to account for the configuration details, the tubulin interaction and various deformation patterns (Fig.1c) of 13-3MTs at the nanoscale.

In the molecular mechanics, the force field is expressed in the form of steric potential energy. The major parts of the steric potential energy of an MT structure include the bond stretching energy U_i^r, the angle bending energy U_i^φ and the dihedral angle torsional potential energy U_i^τ. The total potential energy U of an MT reads

$$U_{bonds}=\sum_{i=1,2}\left(\sum U_i^r+\sum U_i^\varphi+\sum U_i^\tau\right) \tag{1}$$

where i denotes the types of bonds mentioned above (i=1 for the intra-PF bonds and i=2 for the inter-PF bonds). The expressions for the three types of bond energy are as follows.

$$U_i^r=\frac{1}{2}k_i^r(\Delta r_i)^2,\ U_i^\varphi=\frac{1}{2}k_i^\varphi(\Delta\varphi_i)^2,\ U_i^\tau=\frac{1}{2}k_i^\tau(\Delta\Phi_i)^2,(i=1,2) \tag{2}$$

Here, as shown in Fig. 1c, Δr_i is the change of bond length, $\Delta\varphi_i$ is the change of in-plane bond angle, $\Delta\Phi_i$ is the change of out-of-plane angle, k_i^r is the force constant for bond stretching, k_i^φ is the force constant for bond angle bending and k_i^τ is the force constant for bond torsion. The values of these force constants can be obtained in atomistic simulations or experiments.

Also, the total potential energy of the MSM model can be written as:

$$U_{beams}=\sum_{i=1,2}\left(\sum U_i^A+\sum U_i^M+\sum U_i^T\right) \tag{3}$$

where, U_i^A is the strain energy of a beam in tension, U_i^M is the strain energy due to bending, U_i^T is the strain energy due to torsion and i specifies the quantities of beam i (i=1 for longitudinal beams and i=2 for lateral beams). The beam energy is calculated by using the formulae below.

$$U_i^A=\frac{1}{2}\frac{Y_iA_i}{l_i}(\Delta l_i)^2,\ U_i^M=\frac{1}{2}\frac{Y_iI_i}{l_i}(2\Delta\alpha_i)^2,U_i^T=\frac{1}{2}\frac{S_iJ_i}{l_i}(\Delta\beta_i)^2,(i=1,2) \tag{4}$$

As shown in Fig. 1d, Δl_i is the length change of the beam, $\Delta\alpha_i$ is the bending angle, $\Delta\beta_i$ is the torsion angle, $Y_i\,A_i$ is the extensional stiffness, $Y_i\,I_i$ is the bending stiffness and S_iJ_i is the torsional

stiffness of the beams.

The equivalency of the MT structure and its MSM model can be established when the corresponding energies in Eqs. 2 and 4 are equal, which leads to the following relationship between the force constants of the bonds and the stiffnesses of the space beams.

$$\frac{Y_i A_i}{l_i} = k_i^r, \ \frac{Y_i I_i}{l_i} = k_i^\varphi, \frac{S_i J_i}{l_i} = k_i^\tau, (i=1,2) \tag{5}$$

In this study, the values of k_i^r, k_i^φ, k_i^τ were obtained from the molecular dynamics simulations in [18, 21, 22] and further optimized in [23], i.e., k_1^r=3nN/nm, k_1^φ=2nN·nm, k_1^τ= 0.04nN·nm, k_2^r=0.14nN/nm, k_2^φ=0.085nN·nm, k_2^τ=0.0017nN·nm. Then, the values of the beam stiffnesses required in the MSM simulations of 13-3MTs can be obtained by using Eq. (5). The MSM model was employed to perform the simulations on the electromechanical vibration of 13-3 MTs.

2.2 Excitation and damping of MT vibrations

The migration of individual MTs in an EF has been observed via video contrast microscopy [3]. In this process, the magnitude of the unbalanced negative charge carried by tubulins was found to be lower than the theoretical one due to the effects of the electroosmotic flow and the surrounding substances [3]. Also, the magnitude varies from one experiment to another [3, 24-26]. On the other hand, the computer simulations from crystallographic data gave an identical value of -5 electron charges for the tubulin monomer isolated from environment [3, 27, 28]. As such, the charge carried by one monomer was set to q = -5e [28] in the present work. Fig. 2 shows an alternating EF generated by a Hertzian Dipole in a spherical polar coordinate system characterised by the radial (r), polar angle (θ) and azimuthal angle (Ψ) coordinators. The math description of the EF can be found in [29-31]. Herein,

we have placed a 13-3 MT (1 μm in length) at a point with $\theta = 0$ and $r = 0.1$m, and the axial direction of the MT is in either azimuthal angle direction $\hat{\Psi}$ (the unit vector) or polar angle direction $\hat{\theta}$ (Fig. 2). When the radial distance r of the MT is much greater than its length, the EF can be approximated as a uniform EF exhibiting harmonic time dependence. The amplitude of the EF is set to $|\vec{E}| = 20$ V/m.

Here, Fig. 2 graphically illustrates a prototype design of MT-based biosensors where an alternating EF is generated by an electronic device (represented by a dipole here) and used to excite the vibration of individual MTs which are a distance away from the electronic device. The frequency shifts of MTs can then be employed as a biomarker to monitor the changes of MT structure and stiffness in pathological and physiological processes. Thus, the distance $r = 0.1$ m is selected here between the dipole and MTs to demonstrate such a design of the MT-based biosensor. In the meantime, it is understood that the amplitude of time-dependent EF should be large enough to excite the forced vibration of MTs with sufficiently large amplitude and thus, easy to identify by e.g., vibration energy absorption. The safety is another issue that needs to be taken into consideration. $|\vec{E}| = 20$ V/m was selected here as it is relatively strong but safe for human being according to World Health Organization and Federal Office for Radiation Safety, Germany [32]. In addition, the fixed-fixed end conditions were imposed on the 13-3 MT in Fig. 2. The vibrations of the MT are stimulated by the alternating EF via the corresponding electrical force $\vec{F} = \vec{E}q$ on MT tubulins. In this study, the vibration analysis was carried out based on the MSM model [18] developed for 13-3MTs as shown above. The details of the mathematic techniques used in vibration analyses are introduced in the Supplementary Material.

Moreover, a parametric study is conducted for the transverse vibration of MTs in cytosol across a range of damping effects and the frequencies up to 50 MHz. The damping force F_d on the MT

monomers is used to characterise the energy dissipation in viscous flow of cytosol and calculated based on the slide film damping theory accounting for the damping effect of microfluid between two moving microscale objects [33, 34]. First, a non-slip boundary condition associated with a continuous MT-cytosol interface was considered in calculating F_d. After that, damping reduction coefficient P from 0.0001 to 0.1 was introduced to estimate the reduced damping effect. i.e., the damping force on the monomers decreases to $F_{Rd} = F_d \times P$. Here it should be pointed out that these calculations provide insights into how much reduction is required to achieve prominent MT vibration in cell. However, the possible damping reduction due to the relative sliding [14] and the vdW interaction between MT and cytosol needs to be evaluated in future study based on experiments or atomistic simulations. The details of the theory and the damped model are shown in Supplementary Material. Meanwhile, the quality factor $Q = \omega_m / \Delta\omega$ is also calculated for the damped MT vibration, where ω_m is the frequency at the maximum amplitude, A_m is the amplitude of the resonance peak and $\Delta\omega$ is the frequency increment at the points with amplitude $A_m/\sqrt{2}$. [35, 36].

3. Results and discussions

In this section, the forced vibrations of MTs subject to an alternating EF were explored, and the influence of the abnormal interaction between adjacent tubulins was examined. In addition, a parametric study was also conducted to evaluate the influence of the reduced cytosol damping due to the distinctive MT-cytosol interface at the nanoscale.

3.1 Electromechanical vibrations

3.1.1 Vibrations excited by transverse electric field

As mentioned in Sec. 1, the investigations on the free vibration of MTs have achieved multiple progresses [10, 11, 37]. The Eigenvalue vibration analysis was efficiently used to predict the vibration modes and resonant frequencies of MTs [10, 13, 20]. The associated vibration amplitude however cannot be obtained by solving the Eigenvalue problems. In this study, we further studied the forced vibrations of MTs excited by a uniform EF. The major concerns are (1) the possible vibration modes and associated frequencies that can be excited by an alternating EF in the transverse or axial direction of MTs, and (2) "vibration amplitude-EF frequency" relations, which is crucial in predicting the equivalent dipole moment of vibrating MTs [6] and facilitating the design of MT-based biosensors based on the electromechanical vibration of MTs [14].

First, the forced vibrations of MTs excited by the transverse alternating EF (Fig. 2) are presented in Fig. 3 in comparison with the free vibrations obtained for the same MT via the Eigenvalue analysis. The top panel of Fig. 3 shows seven transverse free vibrations whose resonant frequency up-shifts with the growing half wavenumber and falls in the range of (0MHz, 250MHz). The amplitudes of the MT are measured at the three points whose distance from the left MT end is $L/2$, $L/4$ and $L/8$, respectively (L is the MT length) (Fig. 3). In the obtained amplitude-frequency spectra (Fig. 3) seven peaks were picked up in the vicinity of the resonant frequencies. Accordingly, seven forced transverse modes were achieved, which are identical to the seven free vibration modes shown in Fig. 3. Meanwhile, for a given amplitude the bandwidths of the peaks (the frequency span around the frequency peak with the amplitude greater than the given value) associated with the odd half wavenumbers 1, 3, 5 and 7, are

found to be greater than those corresponding to the even half wavenumbers 2, 4 and 6. In addition, among the peaks with an odd half wavenumber, the bandwidth increases with decreasing wavenumber or declining frequency. The observation suggested that the excitation of the MT vibration with relatively large odd half-wavenumber and particularly, even half-wavenumbers are very sensitive to the selected frequency of the EF, and accordingly, showed narrow or sharp peaks in the amplitude-frequency spectra. They can be obtained only if the frequency of excitation is the same as the corresponding resonant frequency of MTs. A small deviation from the resonant frequency would extinguish these even modes. It follows that the odd transverse modes of MTs with low frequency can be excited in a wider range of frequency and thus, are promising for their applications in the MT-based biosensors.

3.1.2 Vibrations stimulated by axial electric field

Possible vibration behaviours of MTs other than transverse modes have been predicted by Eigenvalue analysis [6, 10]. Such vibration modes can also be achieved by applying an alternating EF in the axial direction (Fig. 4a). Fig. 4b, c and d show the three typical examples and the associated amplitude-frequency spectra. The radial breathing mode (RBM) with a circular cross-section and the axial half wavenumber m =1 was observed at around 53.019MHz (Fig. 4a). In RBM, the α and β tubulins of the MT oscillate in the radial direction as if the MT was breathing with a time-dependent radius. The vibrational radial displacement is distributed uniformly along the perimeter of MT cross section. Along the MT length, the distribution however becomes non-uniform and characterised by the axial half wavenumber m, which increases with rising frequency. For instance, the frequency 159.291MHz of the RBM with m = 3 is three times as much as the 53.019MHz associated with m = 1.

In addition, the circumferential modes with a non-circular cross-section [11, 38] was also found in Fig. 4c at around 585.64 MHz. The radial amplitudes (Fig. 4a) at the middle point of the MTs were recorded in the amplitude-frequency spectra for the vibration modes (Fig. 4b and c). Here, two peaks are observed around the resonance frequencies (of RBMs) 53.019MHz (Fig.4b) and 585.64 MHz (Fig.4c), respectively. The amplitude is of the order of 0.02nm at 53.019 ± 0.001MHz and 0.0003nm at 585.64 ± 0.001MHz, which is two orders of magnitude smaller than the first one. Meanwhile, in Fig. 4c another peak of circumferential mode was also observed at a frequency slightly lower than 585.64 MHz of RBM.

Herein, it is worth mentioning that for a nanostructure, factors other than the vdW interface and the sliding between MT and cytosol may also have influence on the damping of surrounding water. For example, in [39] the wettability of water and especially, the slip length are identified as major factors affecting water damping effect on the longitudinal vibration of polarized nanorods.

In addition to RBMs, the axial vibration mode at around 377.84 MHz possesses the highest amplitude as shown in Fig. 4d. Specifically, a sinusoidal alternating EF with an amplitude of 20V/m can excite the axial vibration of individual MTs with a bandwidth (associated with amplitude greater than 0.1nm) around 150 KHz, i.e., from 377.915MHz to 377.765MHz. In this study, the amplitude 0.1nm is selected as a reference oscillatory displacement. The bandwith of a resonant peak is then defined as the frequency range (around the peak) associated with the amplitude greater than 0.1nm. This definition allows us to compare the bandwith between different resonant peaks [6].

3.2 Dependence of vibration on tubulin interaction

It was shown recently [40] that cell stiffness can be used as a biomarker to identify cancerous cells among surrounding healthy cells. Herein, MTs are known as one of the major structural elements responsible for cell stiffness and the variation of MT stiffness can be reflected by the frequency shift of MT vibration excited by an EF [14]. It is thus expected that MT frequency can be used as a bio-indicator to quantify the changes in the structural stiffness of MTs in diseased cells.

It is understood that the structural domains of tubulins, i.e., the N-terminal, intermediate, and C-terminal domains [41], may contribute to heterodimer stability, longitudinal and lateral PF interactions, nucleotide exchange and hydrolysis, and MT–protein interactions [41]. Disease-causing amino acid substitutions are found among the three domains of tubulins and therefore predicted to perturb a range of MT functions [42]. Specifically, the disease-causing substitutions in TUBB2B alter amino acids in domains important for GTP binding, heterodimer stability and longitudinal interactions, and those in TUBB3 are located primarily in regions that regulate GTP binding, heterodimer stability, and longitudinal and lateral interactions. It follows that the variation of MT stiffness may arise from the abnormal interactions between adjacent tubulins due to pathological changes (e.g., the above-mentioned disease-causing substitutions or the cancer progression induced structural remodelling of MTs) in human body [23]. It is thus of great interest to study the dependence of the elastic moduli and vibration frequency of MTs on the strength of tubulin interaction. The outcomes have potential applications in developing biosensor for the biophysical properties of individual MTs or cells.

To mimic this scenario, we have adjusted the strength of longitudinal and helical tubulin interactions by varying the values of the force constants k_i^r, k_i^φ, and k_i^τ (Sec.2.1) that control changes

in the bond length, the bond angle and the dihedral angle of tubulin interactions (Fig.1c and d). k_i^r, k_i^φ, and k_i^τ for normal cells were obtained in [21, 23] and replaced in this study by Ωk_i^r, Ωk_i^φ, and Ωk_i^τ where Ω is a coefficient ranging from 0.2 to 2, which allows us to produce the elastic modulus close to the experimentally obtained stiffness of cancer cells at different progression stages [40]. First, Young's modulus Y and Shear modulus G are measured for the MTs where the strength of the tubulin interactions varies by an order of magnitude. The method used here to measure the elastic moduli is demonstrated in [18]. Subsequently, the fundamental vibration is studied for the above MTs subject to a transverse EF. The aim of this study is to establish the correlation between the tubulin interaction and the bandwidth at the resonant frequency, which is defined by the frequency span with an amplitude greater than 0.1nm [6].

As shown in Fig. 5a, when the longitudinal interaction is altered with Ω rising from 0.2 to 2, G changes slightly around 1.5MPa [43], while Y increases linearly from 0.17GPa to 1.71GPa by a factor of 10.06. In the same process, the fundamental frequency rises from 9.02MHz to 23.67MHz (by a factor of 2.62) while the bandwidth decreases from 7.05MHz to 2.48MHz (by 65%). The trend of the properties and dynamic responses to change with helical interaction is plotted in Fig. 5b. In contrast to the longitudinal interaction effect, Y remains nearly unchanged while G grows linearly from 0.32MPa to 2.86MPa by a factor of 8.94 with rising Ω. It also is noted in Fig.5b that when Ω rises from 0.2 to 2, the fundamental frequency rises from 13.67MHz to 19.41MHz (by 42%) while the bandwidth decreases from 4.30MHz to 3.03MHz (by 30%). The effect of the helical interaction on the frequency and the bandwidth is found to be smaller than the effect of the longitudinal interaction.

Herein, the longitudinal interaction is found to be important for axial Young's modulus, while the

helical interaction is mainly responsible for Shear modulus. These results are in agreement with [23, 44]. In consistent with this observation, the longitudinal interaction also plays a major role in fundamental (transverse) vibration, where axial Young's modulus has a predominant effect over shear modulus. Moreover, the fundamental frequency also changes with the variation of the helical interaction and is found to be more sensitive to the helical interaction weakening than its strengthening. For instance, when Ω falls from 1 to 0.2, i.e., the helical interaction is weakened by 80%, the fundamental frequency decreases by 26% while it only increases by 5% when Ω rises from 1 to 2, i.e., the helical interaction is strengthened by 100%.

The above study indeed shows a typical example that the nanostructures of subcellular components like MTs may have a substantial influence on their overall static and dynamic responses [1]. The prominent role of longitudinal interaction in the transverse MT vibration originates from its influence on axial Young's modulus that controls the bending or transverse deformation of MTs. In the meantime, the helical interaction is responsible for the resistance of MTs to shear deformation or inter-PF sliding. Weakening the helical interaction leads to significant inter-PF sliding [19, 23, 45], which however is prohibited when the interaction is strengthened. This explains the relatively large frequency shift due to the helical interaction weakening. These results obtained in the present simulations show the potential of polarized MTs as a biosensor and its frequency as a possible biomarker in detecting the property and structural changes in individual MTs or cells in physiological or pathlogical processes.

3.3 Evaluation of reduced cytosol damping

In previous sections, the EF-excited vibrations of individual MTs are investigated without

considering any damping effect in the intracellular environment. In reality, MTs are submerged in cytosol of cells (70% water). Thus, cytosol damping cannot be avoided. On the other hand, cytosol damping may reduce to some extent due to, e.g., the possible MT-cytosol sliding and the vdW interaction although we are still waiting for experiments or simulations to confirm this assumption. Therefore, it is of interest to conduct a parametric study of cytosol damping and find the condition under which the prominent vibration of MTs can be excited by EF. It was shown in Sec.2 that a coefficient P was introduced to decrease the frictional forces on the MT due to surrounding cytosol and thus, measure the reduction of the damping effect. The amplitude-frequency spectra are calculated in Fig. 6 for the transverse vibrations with P rising from 0.0001 to 1. For the continuous MT-cytosol interface with $P = 1$, viscous damping is so strong that can extinguish the vibrations of MTs, which is found to be in agreement with [46]. When the damping effect decreases to $P = 0.1$, the amplitude increases but is still very small. Further decreasing P to 0.01, 0.001 and to 0.0001 leads to the increasing amplitude of the order of 0.02 nm, 0.2 nm and 1.2 nm, respectively. Thus, transverse vibration with amplitude greater than 0.1nm [6] can be achieved when the cytosol damping effect can decrease by three orders of magnitude due to the unique features of the MT-cytosol interface at the nanoscale. To reveal the trend of quality factor Q in this process we have calculated the frequency spectra with P ranging from 0.002 to 0.009 in the inset of Fig. 6. In the figure, Q is found to increase with decreasing damping effect measured by P and at $P < 0.003$ $Q > 4.3$ can be obtained. Here, it is worth mentioning that decreasing cytosol damping leads to greater Q mainly by raising the amplitude. In this process, the bandwidth also grows with increasing Q or decreasing P. Thus, reduced cytosol damping makes it easier for one to excite a transverse vibration of MTs in cells.

Here, it should be noted that the present study evaluates the reduction of cytosol dmaping required to stimulate prominent vibration of MTs in cells. It is however not celar whether the unique MT-cytosol interface can finally achieve the goal. In addition, the experimental evidence of MT vibration in cells is still not available in the literature. There are two possibilities, i.e., (1) The MT-cytosol interface cannot substantially decrease the damping effect of cytotol which finally quenches the vibrations of MTs in cells. (2) More advanced signal acquisition technique is required to indentify the resonance of nanoscale components of cells and tissues. Indeed, these issues as well as many other technique challenges need to be addressed before one can eventually realise the proposed MT-based biosensors.

4. Conclusions

In the present paper, an alternating EF was used to excite the forced vibration of polarized MTs in different modes. The possibility was also examined to detect the abnormal tubulin interaction in the pathological process by measuring the changes in the frequency and elastic moduli of MTs. The effect of cytosol damping is also evaluated for the transverse vibration of the MT.

It is found that a transverse EF is able to excite transverse vibrations of MTs where frequency upshifts from 18.4 to 240.3 MHz when the half axial wavenumber rises from one to seven. The vibrations with the even half wavenumbers are hard to excite as they show a very narrow bandwidth on the vibration spectra, while it is relatively easy to achieve those with odd half wavenumber due to their much wider bandwidth which increases with the decreasing frequency.

An axial EF is found to generate RBMs (with a circular cross-section) of MTs, which can be

observed in the vibration spectra at a frequency around 53.019 MHz and 159.291 MHz, much higher than the frequencies of the transverse vibrations with the same half axial wavenumber. The circumferential vibrations with non-circular cross-section are also achieved at 585.64 MHz. In addition, the axial vibration of frequency 377.84 MHz can also be excited, where the amplitude is found to be greater than other modes stimulated by an axial EF.

For MTs in cells, the excitation of prominent vibrations depends largely on the possible MT-cytosol sliding at the interface, which may substantially reduce cytosol damping. The transverse vibration with amplitude greater than 0.1nm and quality factor Q larger than 4.3 can be achieved by applying an EF of 20 V/m provided that the sliding MT-cytosol interface can largely decrease the damping by three orders of magnitude relative to the cytosol damping due to a normal continuous MT-cytosol interface.

In addition, it is also found that the longitudinal tubulin interaction determines the axial Young's modulus that controls the bending deformation or the transverse vibration, while the helical tubulin interaction mainly decides shear modulus and the inter-PF sliding. Thus, changes in the longitudinal or helical interaction in pathological processes can be detected via the variation of elastic moduli and the shift of MT frequency as promising biomarkers.

Indeed, correlating the pathological changes of MTs to their responses to an alternating EF is crucial for the development of MT-based biosensors. Hence, the dependence of MT frequency on the tubulin interaction achieved here not only reveal the structure-property relation of MTs, but also provides useful guidance to the development of the MT-based biosensors to detect the changes in the mechanical properties and strcutres of individual MTs or cells.

Competing interests

We have no competing interests.

Acknowledgements

S. Li acknowledges the financial support from the China Scholarship Council (CSC) and College of Engineering, Swansea University.

References

[1] Howard, J. & Hyman, A.A. 2003 Dynamics and mechanics of the microtubule plus end. *Nature* **422**, 753-758. (doi:10.1038/nature01600).

[2] Barzanjeh, S., Salari, V., Tuszynski, J., Cifra, M. & Simon, C. 2017 Optomechanical proposal for monitoring microtubule mechanical vibrations. *Phys Rev E* **96**, 012404. (doi:10.1103/PhysRevE.96.012404).

[3] Stracke, R., Böhm, K., Wollweber, L., Tuszynski, J. & Unger, E. 2002 Analysis of the migration behaviour of single microtubules in electric fields. *Biochem. Biophys. Res. Commun.* **293**, 602-609. (doi:10.1016/S0006-291X(02)00251-6).

[4] Nogales, E., Wolf, S.G. & Downing, K.H. 1998 Structure of the αβ tubulin dimer by electron crystallography. *Nature* **391**, 199-203. (doi:10.1038/30288).

[5] Pizzi, R., Strini, G., Fiorentini, S., Pappalardo, V. & Pregnolato, M. 2011 Evidences of new biophysical properties of microtubules. In *Artificial Neural Networks*

Engineering tools, techniques and tables

Mathematics research developments series (ed. S.J. Kwon), Nova Science Publishers.

[6] Cifra, M., Pokorný, J., Havelka, D. & Kučera, O. 2010 Electric field generated by axial longitudinal vibration modes of microtubule. *BioSyst.* **100**, 122-131. (doi:10.1016/j.biosystems.2010.02.007).

[7] Sirenko, Y.M., Stroscio, M.A. & Kim, K. 1996 Elastic vibrations of microtubules in a fluid. *Phys Rev E* **53**, 1003. (doi:10.1103/PhysRevE.53.1003).

[8] Pokorný, J. 2003 Viscous effects on polar vibrations in microtubules. *Electromagn. Biol. Med.* **22**, 15-29. (doi:10.1081/JBC-120020349).

[9] Kasas, S., Cibert, C., Kis, A., Rios, P.L., Riederer, B., Forro, L., Dietler, G. & Catsicas, S. 2004 Oscillation modes of microtubules. *Biol. Cell* **96**, 697-700. (doi:10.1016/j.biolcel.2004.09.002).

[10] Wang, C.Y., Ru, C.Q. & Mioduchowski, A. 2006 Vibration of microtubules as orthotropic elastic shells. *Physica E* **35**, 48-56. (doi:10.1016/j.physe.2006.05.008).

[11] Wang, C.Y. & Zhang, L.C. 2008 Circumferential vibration of microtubules with long axial wavelength. *J. Biomech.* **41**, 1892-1896. (doi:10.1016/j.jbiomech.2008.03.029).

[12] Arani, A.G., Abdollahian, M. & Jalaei, M. 2015 Vibration of bioliquid-filled microtubules embedded in cytoplasm including surface effects using modified couple stress theory. *J. Theor. Biol.* **367**, 29-38. (doi:10.1016/j.jtbi.2014.11.019).

[13] Li, S., Wang, C.Y. & Nithiarasu, P. 2017 Three-dimensional transverse vibration of microtubules. *J. Appl. Phys.* **121**, 234301. (doi:10.1063/1.4986630).

[14] Pokorný, J., Vedruccio, C., Cifra, M. & Kučera, O. 2011 Cancer physics: diagnostics based on damped cellular elastoelectrical vibrations in microtubules. *Eur. Biophys. J.* **40**, 747-759. (doi:10.1007/s00249-011-0688-1).

[15] Deriu, M.A., Enemark, S., Soncini, M., Montevecchi, F.M. & Redaelli, A. 2007 Tubulin: from atomistic structure to supramolecular mechanical properties. *J. Mater. Sci.* **42**, 8864-8872. (doi:10.1007/s10853-007-1784-6).

[16] Enemark, S., Deriu, M.A., Soncini, M. & Redaelli, A. 2008 Mechanical model of the tubulin dimer based on molecular dynamics simulations. *J. Biomech. Eng.* **130**, 041008. (doi:10.1115/1.2913330).

[17] Deriu, M.A., Soncini, M., Orsi, M., Patel, M., Essex, J.W., Montevecchi, F.M. & Redaelli, A. 2010 Anisotropic elastic network modeling of entire microtubules. *Biophys. J.* **99**, 2190-2199. (doi:10.1016/j.bpj.2010.06.070).

[18] Zhang, J. & Wang, C.Y. 2014 Molecular structural mechanics model for the mechanical properties of microtubules. *Biomech. Model. Mechanobiol.* **13**, 1175-1184. (doi:10.1007/s10237-014-0564-x).

[19] Chrétien, D. & Fuller, S.D. 2000 Microtubules switch occasionally into unfavorable configurations during elongation. *J. Mol. Biol.* **298**, 663-676. (doi:10.1006/jmbi.2000.3696).

[20] Zhang, J. & Wang, C.Y. 2016 Free vibration analysis of microtubules based on the molecular mechanics and continuum beam theory. *Biomech. Model. Mechanobiol.* **15**, 1069-1078. (doi:10.1007/s10237-015-0744-3).

[21] Ji, X.Y. & Feng, X.Q. 2011 Coarse-grained mechanochemical model for simulating the dynamic behavior of microtubules. *Phys Rev E* **84**, 031933. (doi:10.1103/PhysRevE.84.031933).

[22] Zhang, J. & Meguid, S. 2014 Buckling of microtubules: An insight by molecular and continuum mechanics. *Appl. Phys. Lett.* **105**, 173704. (doi:10.1063/1.4900943).

[23] Li, S., Wang, C. & Nithiarasu, P. 2018 Structure–property relation and relevance of beam theories for microtubules: a coupled molecular and continuum mechanics study. *Biomech. Model. Mechanobiol.* **17**, 339-349. (doi:10.1007/s10237-017-0964-9).

[24] Vater, W., Stracke, R., Boehm, K., Speicher, C., Weber, P. & Unger, E. 1998 Behaviour of individual microtubules and microtubule bundles in electric fields. In *Sixth Foresight Conference on Molecular Nanotechnology* (

[25] Vassilev, P.M., Dronzine, R.T., Vassileva, M.P. & Georgiev, G.A. 1982 Parallel arrays of microtubles formed in electric and magnetic fields. *Biosci. Rep.* **2**, 1025-1029. (doi:10.1007/BF01122171).

[26] Vassilev, P. & Kanazirska, M. 1985 The role of cytoskeleton in the mechanisms of electric field effects and information transfer in cellular systems. *Med. Hypotheses* **16**, 93-96. (doi:10.1016/0306-9877(85)90065-9).

[27] Brown, J.A.M. 2000 A Study of the Interactions between Electromagnetic Fields and Microfit ubules: Ferroelect ric Effects, Signal Transduction and Electronic Conduct ion, University of Alberta.

[28] Mershin, A., Kolomenski, A.A., Schuessler, H.A. & Nanopoulos, D.V. 2004 Tubulin dipole moment, dielectric constant and quantum behavior: computer simulations, experimental results and suggestions. *BioSyst.* **77**, 73-85. (doi:10.1016/j.biosystems.2004.04.003).

[29] Grant, I.S. & Phillips, W.R. 2013 *Electromagnetism*. Chichester, John Wiley & Sons.

[30] Zahn, M. 1979 *Electromagnetic Field Theory: a problem solving approach*. New York, John

Wiley & Sons.

[31] Griffiths, D.J. 1999 *Introduction to electrodynamics*. New Jersey, Prentice Hall.

[32] WHO. Electromagnetic fields (EMF). *(available at http://www.who.int/peh-emf/about/WhatisEMF/en/index3.html)*.

[33] Chang, H., Zhang, Y., Xie, J., Zhou, Z. & Yuan, W. 2010 Integrated behavior simulation and verification for a MEMS vibratory gyroscope using parametric model order reduction. *Journal of Microelectromechanical Systems* **19**, 282-293. (doi:10.1109/JMEMS.2009.2038284).

[34] Cho, Y.-H., Kwak, B.M., Pisano, A.P. & Howe, R.T. 1994 Slide film damping in laterally driven microstructures. *Sensors and Actuators A: Physical* **40**, 31-39. (doi:10.1016/0924-4247(94)85027-5).

[35] Liu, X., Civet, Y. & Perriard, Y. 2015 Quality factor and vibration amplitude estimation of a piezoelectric-actuated system using impedance measurements. In *Electrical Machines and Systems (ICEMS), 2015 18th International Conference on* (pp. 1993-1996, IEEE.

[36] Piersol, A.G. & Harris, C.M. 2017 *Harri's Shock and Vibration Handbook Fifth Edition*, Mcgraw-hill.

[37] Wang, C.Y., Zhang, J., Fei, Y.Q. & Murmu, T. 2012 Circumferential nonlocal effect on vibrating nanotubules. *International Journal of Mechanical Sciences* **58**, 86-90. (doi:10.1016/j.ijmecsci.2012.03.009).

[38] Wang, C., Ru, C. & Mioduchowski, A. 2005 Free vibration of multiwall carbon nanotubes. *J. Appl. Phys.* **97**, 114323. (doi:10.1063/1.1898445).

[39] Krivosudský, O. & Cifra, M. 2016 Microwave absorption by nanoresonator vibrations tuned with surface modification. *EPL (Europhysics Letters)* **115**, 44003. (doi:10.1209/0295-5075/115/44003).

[40] Luo, Q., Kuang, D., Zhang, B. & Song, G. 2016 Cell stiffness determined by atomic force microscopy and its correlation with cell motility. *Biochimica et Biophysica Acta (BBA)-General Subjects* **1860**, 1953-1960. (doi:10.1016/j.bbagen.2016.06.010).

[41] Löwe, J., Li, H., Downing, K. & Nogales, E. 2001 Refined structure of αβ-tubulin at 3.5 Å resolution. *J. Mol. Biol.* **313**, 1045-1057. (doi:10.1006/jmbi.2001.5077).

[42] Tischfield, M.A., Cederquist, G.Y., Gupta, M.L. & Engle, E.C. 2011 Phenotypic spectrum of the tubulin-related disorders and functional implications of disease-causing mutations. *Curr. Opin. Genet. Dev.* **21**, 286-294. (doi:10.1016/j.gde.2011.01.003).

[43] Kis, A., Kasas, S., Babić, B., Kulik, A., Benoit, W., Briggs, G., Schönenberger, C., Catsicas, S. & Forro, L. 2002 Nanomechanics of microtubules. *Phys. Rev. Lett.* **89**, 248101. (doi:10.1103/PhysRevLett.89.248101).

[44] Pampaloni, F., Lattanzi, G., Jonas, A., Surrey, T., Frey, E. & Florin, E.L. 2006 Thermal fluctuations of grafted microtubules provide evidence of a length-dependent persistence length. *Proc. Natl. Acad. Sci. U. S. A.* **103**, 10248-10253. (doi:10.1073/pnas.0603931103).

[45] Chrétien, D., Flyvbjerg, H. & Fuller, S.D. 1998 Limited flexibility of the inter-protofilament bonds in microtubules assembled from pure tubulin. *Eur. Biophys. J.* **27**, 490-500. (doi:10.1007/s002490050159).

[46] Foster, K.R. & Baish, J.W. 2000 Viscous damping of vibrations in microtubules. *J. Biol. Phys.* **26**, 255-260. (doi:10.1023/A:1010306216654).

Figures and captions

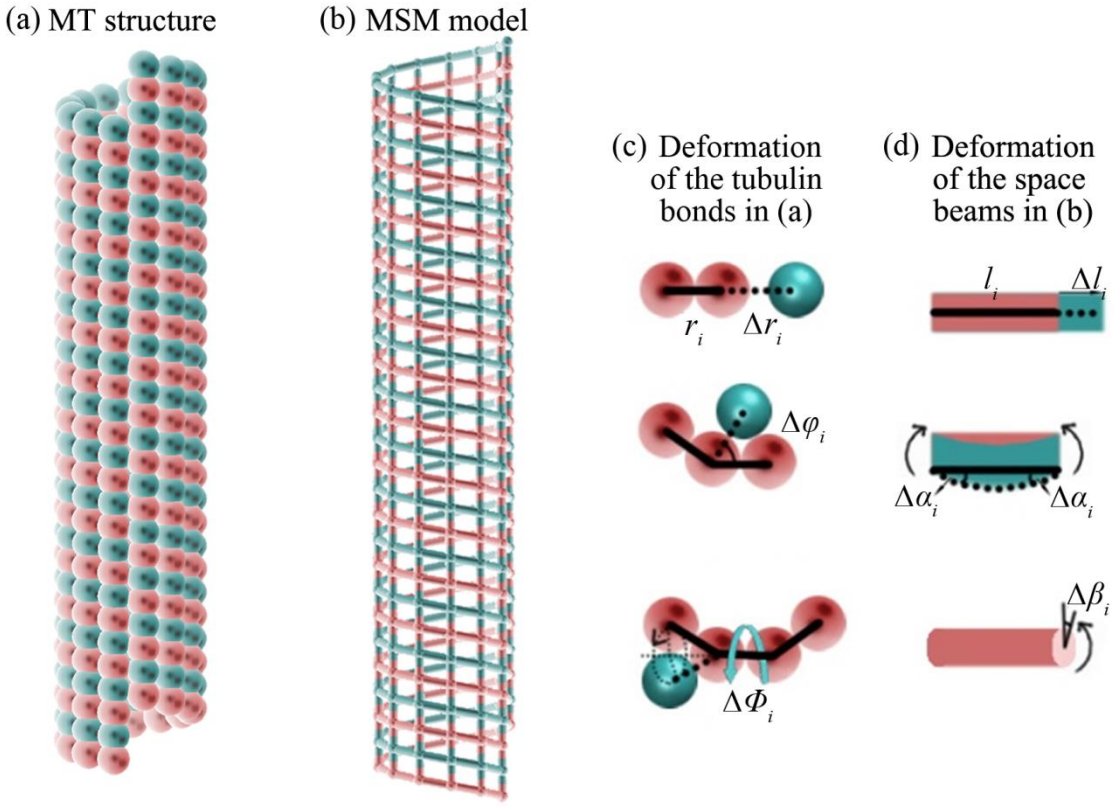

Fig. 1 (a) Structural representation of an MT with tubulin interactions; (b) the MSM model developed for the MT with elastic beams characterising the tubulin interactions; (c) the deformation patterns of the tubulin bonds of the MT and (d) the space beams of the MSM model;

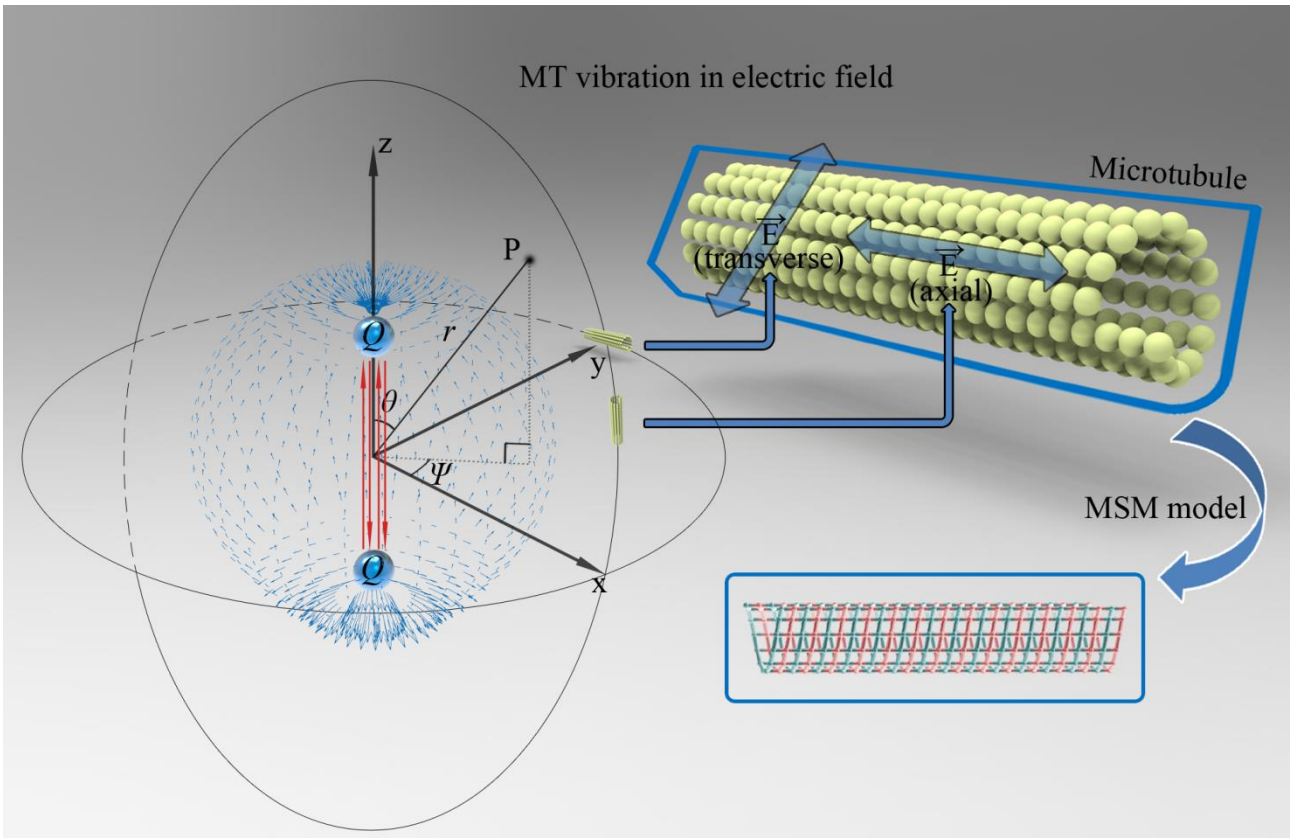

Fig. 2 EF generated by a Hertzian Dipole in a spherical polar coordinate system and its vector directions at the locations where the MTs was placed

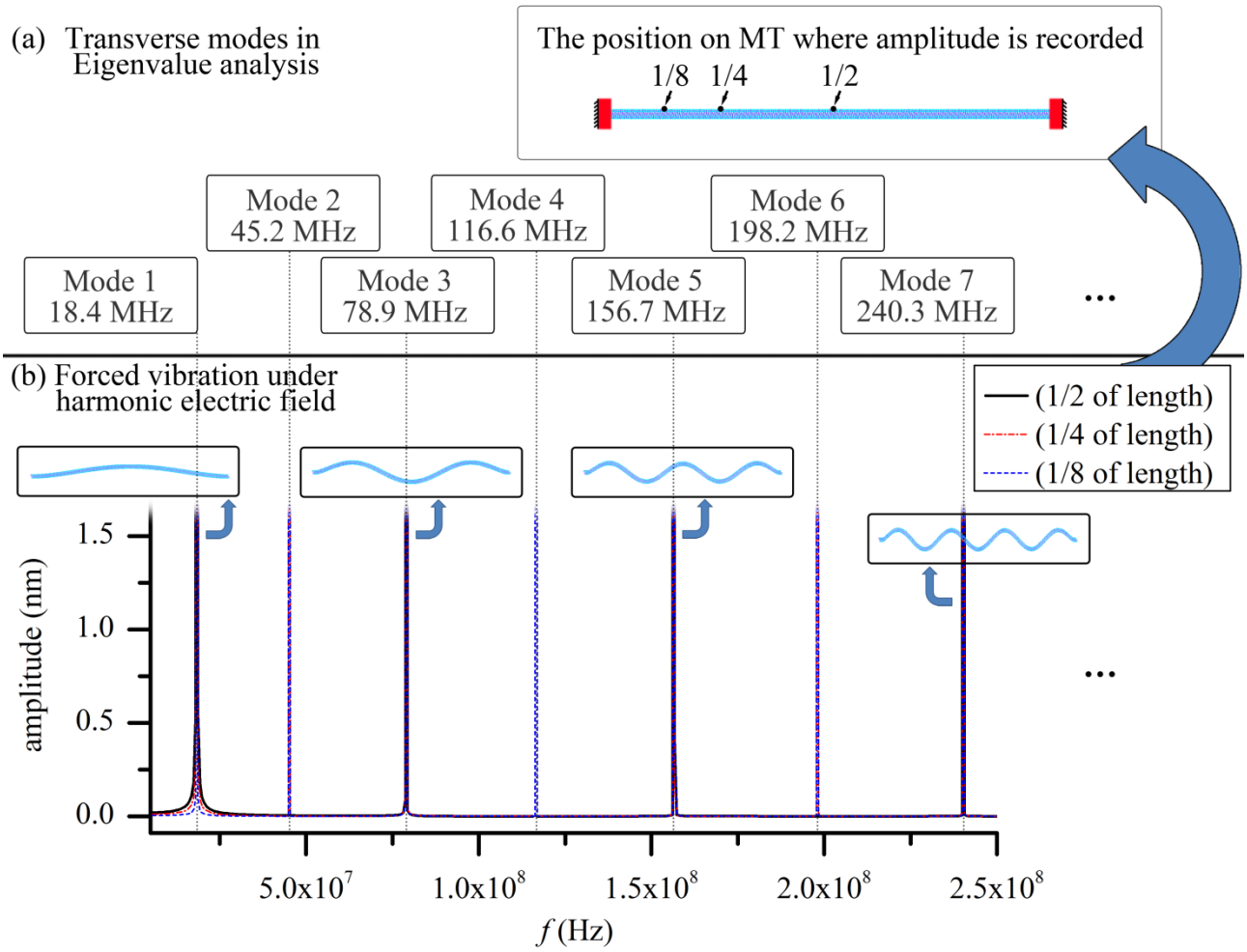

Fig. 3 The comparison between the Eigenvalue transverse vibration modes and the vibrations of MTs excited by the EF in the transverse direction

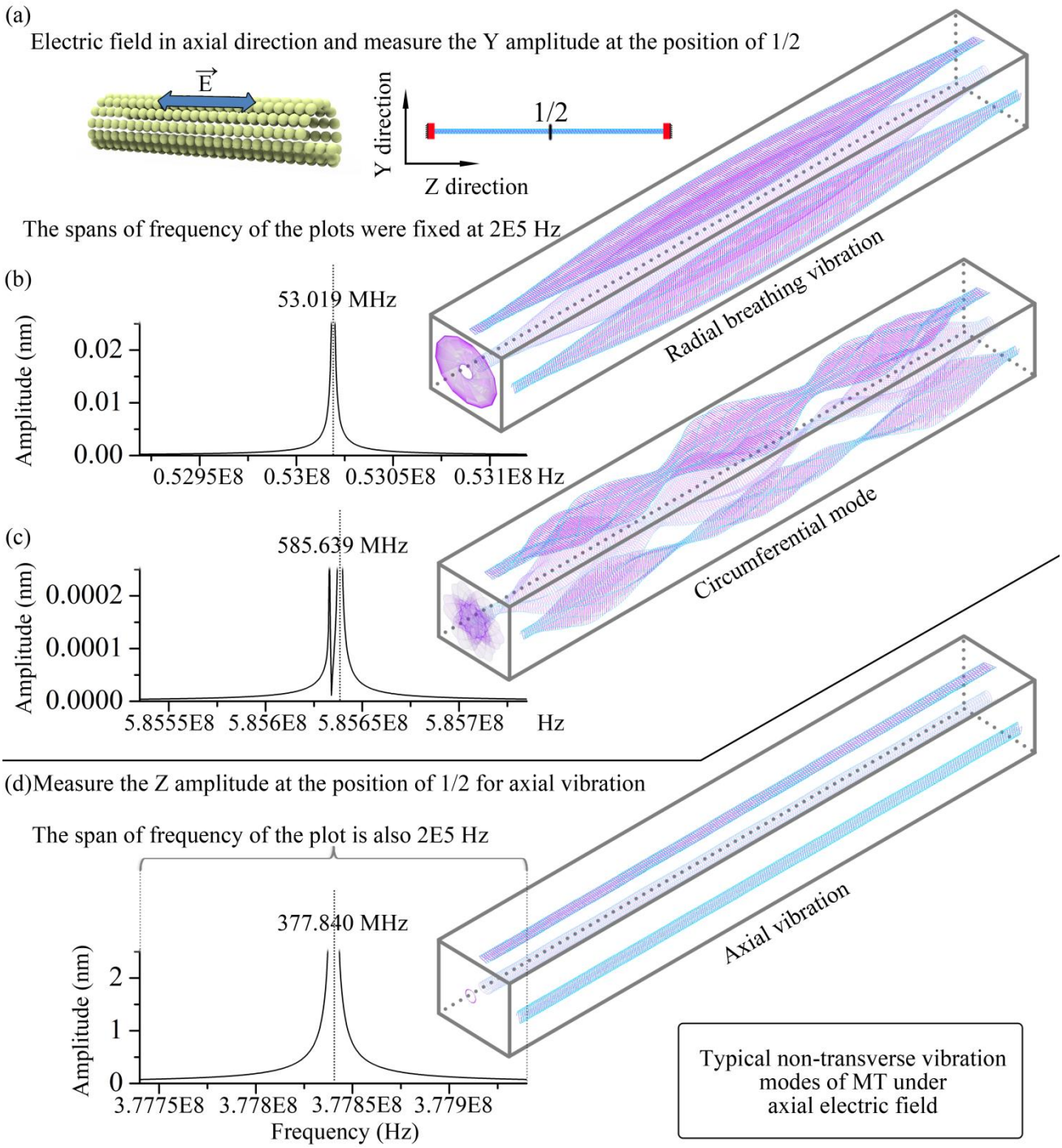

Fig. 4 The vibration modes of MTs excited by the EF in the axial direction

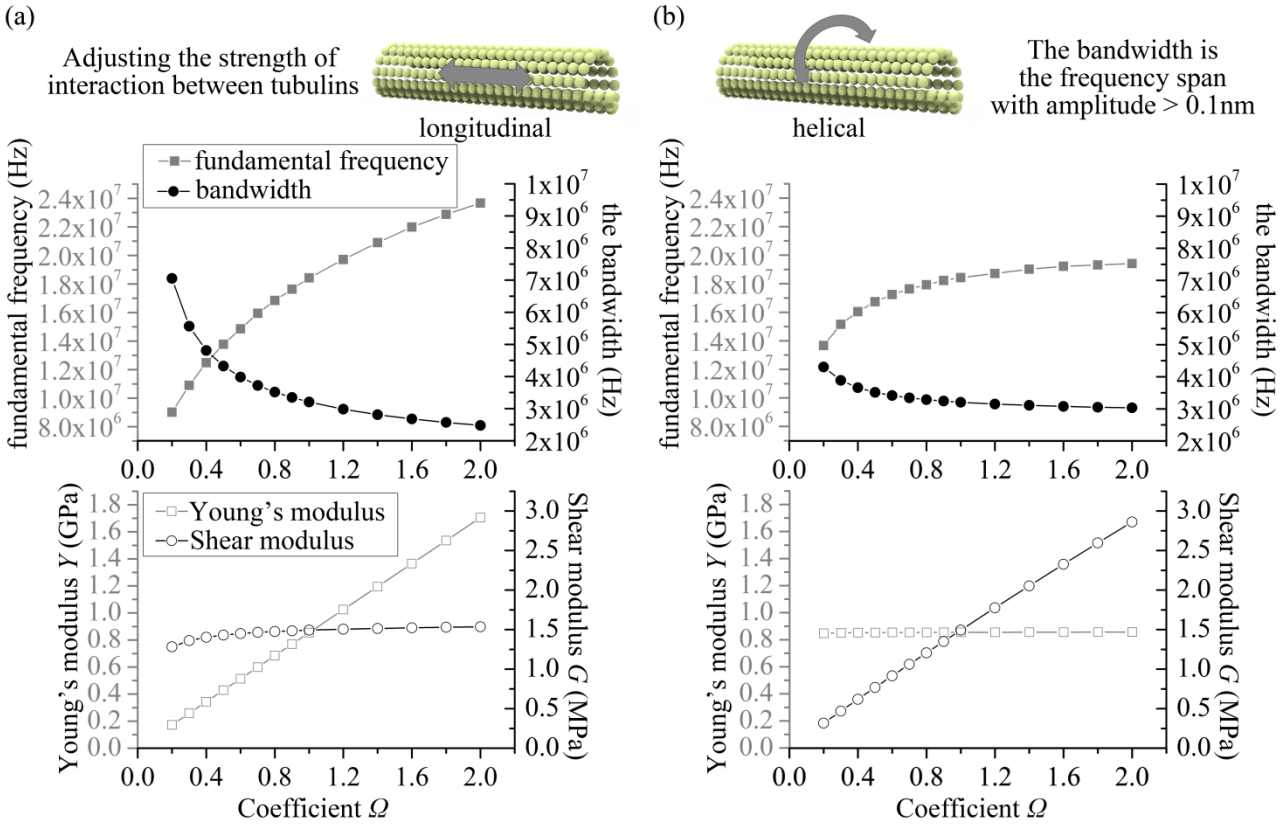

Fig. 5 The changes in vibrational responses and elastic moduli of MTs as a result of (a) abnormal longitudinal interactions between tubulins and (b) abnormal helical interactions between tubulins

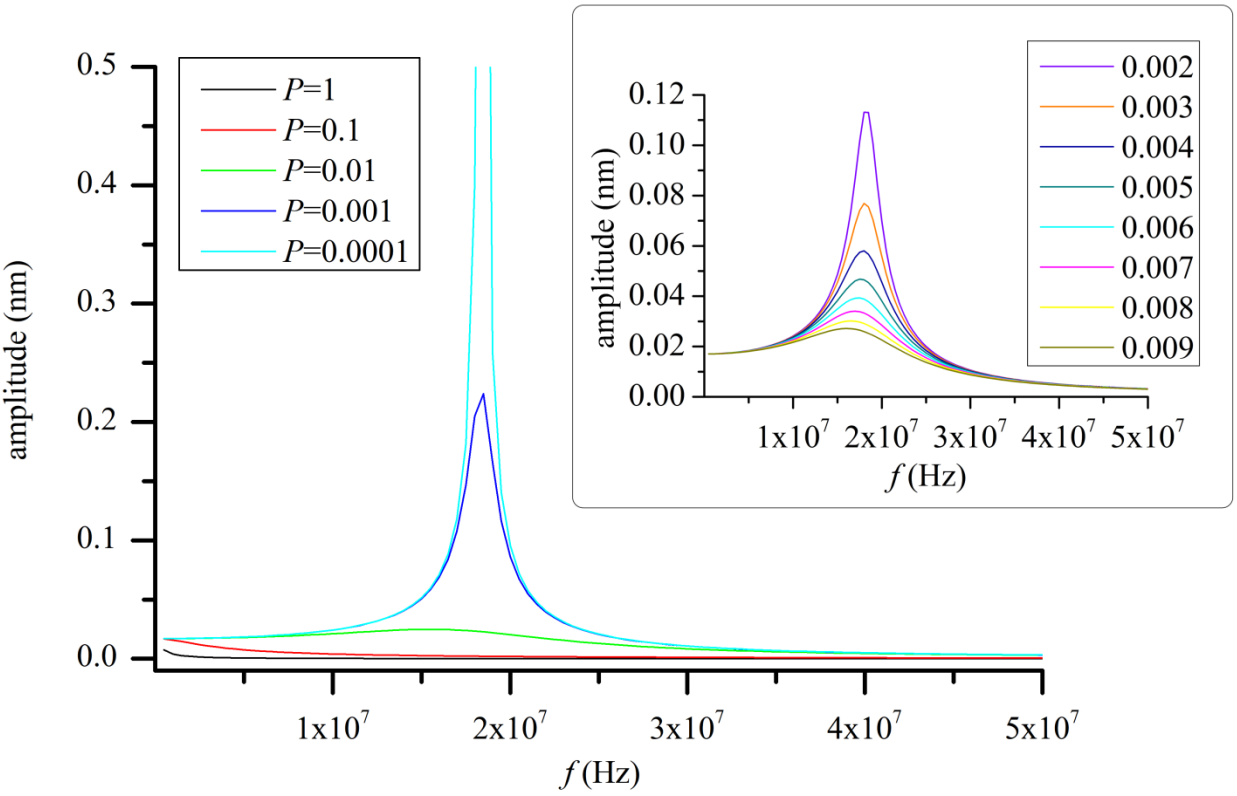

Fig. 6 The changes in responses of damped MT vibration in cytosol due to different damping reduction factors